Available online at www.sciencedirect.com

ScienceDirect

European Journal of Radiology Open 1 (2014) 28–39

EUROPEAN JOURNAL OF RADIOLOGY OPEN

www.elsevier.com/locate/ejro

# MR-PET of the body: Early experience and insights

Miguel Ramalho [a], Mamdoh AlObaidy [a], Onofrio A. Catalano [b], Alexander R. Guimaraes [c], Marco Salvatore [d], Richard C. Semelka [a,*]

[a] *Department of Radiology, University of North Carolina at Chapel Hill, Chapel Hill, NC, USA*
[b] *Department of Radiology, SDN-IRCCS and University of Naples "Parthenope", Naples, Italy*
[c] *Department of Radiology, Massachusetts General Hospital, Boston, MA, USA*
[d] *Department of Radiology, University of Naples "Federico II", Naples, Italy*

Received 1 September 2014; accepted 1 September 2014
Available online 16 September 2014

**Abstract**

MR-PET is a novel imaging modality that combines anatomic and metabolic data acquisition, allowing for simultaneous depiction of morphological and functional abnormalities with an excellent soft tissue contrast and good spatial resolution; as well as accurate temporal and spatial image fusion; while substantially reducing radiation dose when compared with PET-CT.

In this review, we will discuss MR-PET basic principles and technical challenges and limitations, explore some practical considerations, and cover the main clinical applications, while shedding some light on some of the future trends regarding this new imaging technique.


*Keywords:* MR-PET; PET-CT; Whole-body imaging; PET; MRI

## Contents



## 1. Introduction

The development of Magnetic resonance-Positron Emission Tomography (MR-PET) has been a logical next step following the success of Positron Emission Tomography-Computed Tomography (PET-CT). The basis of both approaches is the combination of the relatively low spatial resolution functional information provided by PET superimposed on the higher spatial resolution of a 3D tomographic technique, such as CT or MRI.

* Corresponding author at: Department of Radiology, UNC at Chapel Hill, CB 7510–2001 Old Clinic Bldg., Chapel Hill, NC 27599-7510, USA. Tel.: +1 919 966 9676; fax: +1 919 843 7147.
*E-mail address:* richsem@med.unc.edu (R.C. Semelka).

http://dx.doi.org/10.1016/j.ejro.2014.09.001

The intrinsic qualities of MRI that have driven the development of this combination are the higher intrinsic tissue contrast and the lack of medical radiation.

Since its introduction, hybrid PET-CT has modified the applicability of PET use in clinical practice. The added value of anatomic localization and morphologic characterization provided by CT allowed improved diagnostic accuracy. The advantages of PET-CT, based on hardware-derived registration of the two modalities, has not only largely replaced PET-only scanners in clinical routine, but expanded considerably the clinical and research roles. The major drawback is the high radiation exposure, combining the X-ray radiation of CT with the gamma radiation and radioactive decay of PET.

The success of PET-CT has fostered the interest in using MR as a replacement for CT in a hybrid scanner [1,2]. The anatomical landmarks can also be achieved with MRI, with several potential benefits. These include: improved co-registration of PET and anatomic MR images as MRI data can be simultaneously acquired, unlike the sequential data acquisition with CT; improved soft-tissue contrast resolution compared to CT; and reduction in overall radiation exposure. MRI does not employ ionizing radiation, which is particularly problematic in circumstances of anticipated multiple follow-up studies or in imaging young patients.

MRI provides additional quantitative information regarding tissue function with specific techniques (diffusion, spectroscopy, etc.) and cell-specific contrast agents.

Despite these appropriate rationales, the transition from PET-CT to MR-PET is not simple: the clinical value of PET-CT has already been firmly established, with extensive publications and wide clinical use [3–6]; financial concerns of replacing a very expensive imaging modality with an even more expensive one; the natural tendency of practicing imaging specialists to be hesitant to learn a new modality; and the major technical challenges yet to be resolved, such as the compatibility between PET components and MR magnetic field.

To date, the readout technology (electronics of the PET scintillation detectors) is not MR-compatible; as the photomultiplier-based PET scanners do not readily work within or near the magnetic environment of a MR scanner [7]. MR data, unlike that acquired with CT, are not readily usable for attenuation correction (AC) [8–10], limiting quantification of PET data [11].

In this review we will discuss the imaging aspects and challenges of MR-PET and initial comparison with PET-CT as well as both current and projected clinical applications.

## 2. Photomultipliers in the magnetic environment of MR

Compatibility between the photomultipliers, integral in PET imaging, and MR system has been particularly challenging. A current solution is provided in the Biograph mMR (Siemens medical systems, Erlangen, Germany). In this system, the PET detectors are fully integrated into a 3 Tesla MR system within a single gantry. Photomultipliers were replaced with avalanche photodiode technology, which are less sensitive to magnetic fields. This system design enables simultaneous acquisition of PET and MR data [12–14]. A second method of hybrid MR-PET system uses sequential acquisition mode (Ingenuity TF MR-PET, Phillips, Eindhoven, the Netherlands). However, data acquisition with this system is fundamentally the same as with PET-CT, and sacrifices one of the great advantages that MR-PET can offer, which is simultaneous acquisition.

Simultaneous measurement with MR-PET has been considered one of its strongest features, leading to superior spatial and temporal co-registration of the two modalities; offering a wealth of complementary anatomical, physiological, and molecular information; while considerably shortening scan time compared to separate acquisitions [15].

## 3. Attenuation correction of PET data by MR data

For quantitative PET imaging, the reconstructed data needs to be corrected for γ-photon attenuation. Direct measurement of linear attenuation coefficients is not possible in integrated PET-MR systems. MR information has to be converted to linear attenuation coefficients; however, because the MR signal reflects proton density instead of photon attenuation, this conversion is challenging. As MR does not provide an attenuation map for ionizing radiation, PET data in a MR-PET system cannot be subjected to AC, which renders the PET data qualitative images only. Attenuation correction is mandatory for quantitative assessments with standardized uptake values (SUVs) or radiotracer kinetics [16,17].

Current MR-based attenuation algorithms are founded on the use of a dedicated MRI sequence followed by segmentation-based algorithms to derive three or four tissue classes, excluding bone (see below) [18]. The three-segment model accounts for air, soft tissues, and lungs [16,19]; while the four-segment model accounts for air, soft tissues (muscles and solid organs), fat, and lungs [9]. These models are based on T1-weighted multi-station spoiled gradient echo (GRE) or T1-weighted 2-point Dixon sequences (Fig. 1), respectively. The four-segment model is currently in use in simultaneous Biograph mMR hybrid scanners.

The Dixon sequence divides the body into four distinct tissue types based directly on the MR image intensity. These tissues are then assigned a corresponding linear attenuation coefficient based on known densities. Mineralized bone has a higher linear attenuation coefficient for 511 keV photons than soft tissues but is not represented in Dixon-based MR attenuation methods. Cortical bone has a much faster transverse relaxation rate than soft tissues, and hence any signal produced within traditional MR sequences disappears prior to sampling. As a result, the Dixon-based attenuation correction method does not take cortical bone into consideration and is less robust for osseous lesions [20].

The end product of the Dixon-based technique is four sequences: in-phase, opposed-phase, fat-only, and water-only images. All 4 images are combined to create a μ map, which is used for attenuation correction.

The Dixon sequence is a 20 s duration free-breathing sequence acquired during the first 20 s of the PET scan. Alternative algorithms involving population-based atlases [21], ultra-fast MR sequences for bone derivation [22], or co-registered CT information [23] have been proposed; however,

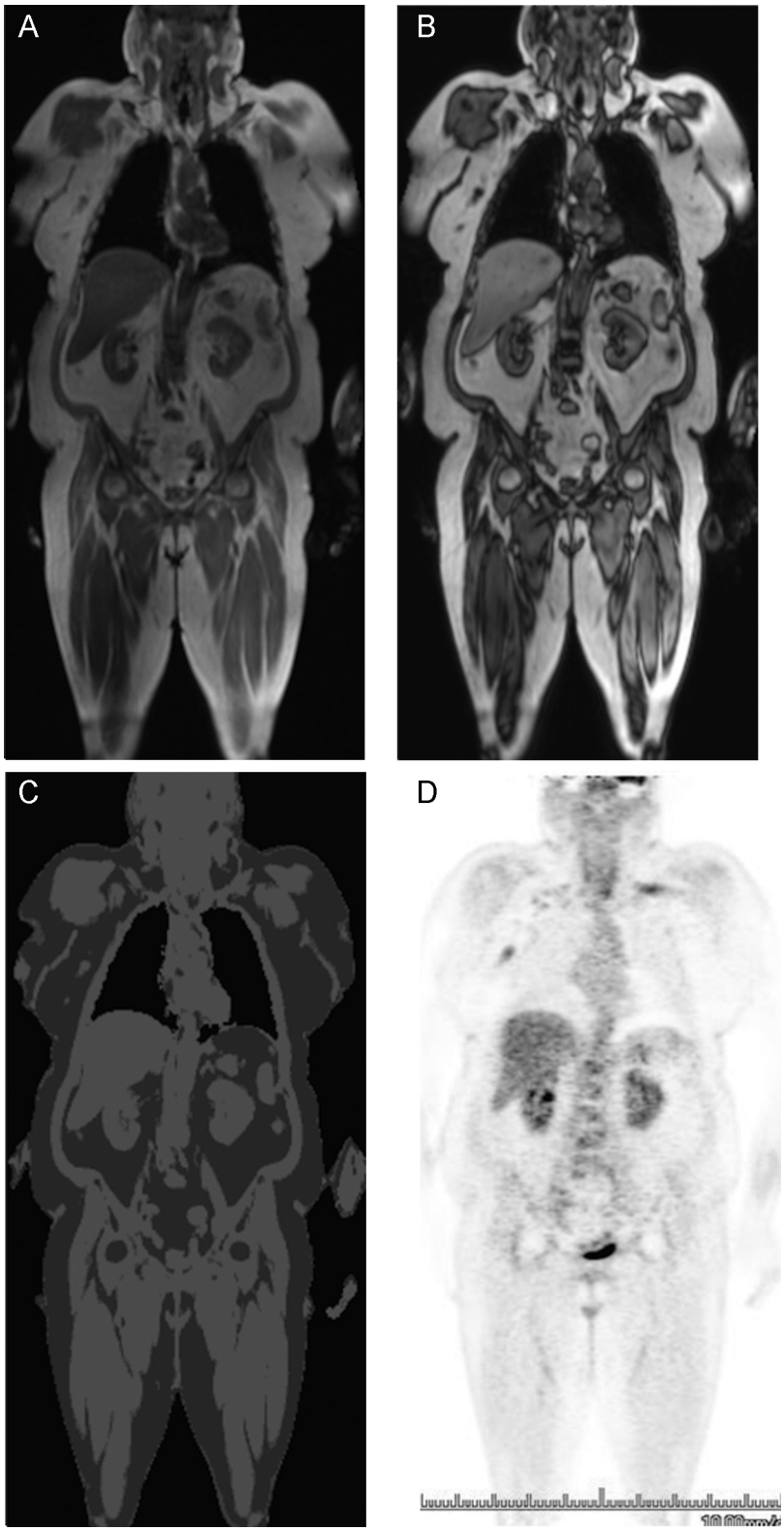


Fig. 1. Soft tissue AC based on MR imaging. In-phase (A) out-of-phase (B) 2-point Dixon images from attenuation correction sequences. Resulting μMap (C) providing separate water/fat images that serve as basis for soft tissue segmentation that can be assigned to a PET attenuation map. Resulting attenuation corrected whole-body PET scan (D).

none of these have yet been adopted into routine MR-PET. AC needs to be improved further, before MR-PET can be used reproducibly for quantitative PET imaging [24].

## 4. MR-PET workflow

A specific challenge in MR-PET is how to develop an optimized workflow. Whole-body MR-PET imaging and sequence optimization must be addressed from a clinical and patient perspective. Whole-body MR-PET should be fast enough to compete with PET-CT (study length approximately 20 min), while providing added clinical value over PET-CT or MRI alone [20].

MR-PET scans take considerably longer than PET-CT scans for a number of reasons. Patient positioning takes longer on the table because coils have to be placed on top of the patient for the MR portion of the examination and MR sequences are longer in duration. Additionally, multiple different data acquisitions are acquired with MRI compared with CT, which employs a single acquisition with faster data accumulation [3]. The tendency of acquiring multiple different types of data acquisitions is a carry-over of MR practice in general. Although this is certainly one of the great strengths of MR and contributes to its superiority over CT in many settings, it comes at the expense of longer study times.

In spite of flexibility seen with diagnostic MRI in general, a specific tailor-designed imaging protocol is recommended in order to be fast enough without compromising the image quality required to achieve high diagnostic accuracy. Another important aspect to tailor MR-PET protocols short is to render the study economical viability.

The imaging protocols and workflow are dependent on the design and the type of the MR-PET unit. In simultaneous MR-PET systems, the image acquisition of PET and MRI can occur concurrently for a given bed position. In the sequential approach, MRI is performed either before or after PET data acquisition. It is important to note that, depending on the type of sequences used, some sequences must run separately from the PET data acquisition in the simultaneous MR-PET systems, as many of the sequences used in body MRI rely on breath-hold acquisitions [25].

To a large extent, as a reflection of the newness of the hybrid modality, there are currently no universally accepted standard protocols for MR-PET [26–29]. Protocols likely will have to be tailored to specific disease entities. For example, in settings where imaging the liver for disease is crucial, dynamic imaging of the liver will be mandatory, as MRI is superior in characterization and detection of liver lesions compared to either CT or PET alone (Fig. 2).

Although most of the organ-based protocols may initially be similar to standard protocols for MRI-only examinations, it will have to be determined to what extent MRI can be condensed to be a "minimum necessary" protocol, with the maximum diagnostic outcome reflecting the addition of PET data [30]. Likewise, advanced MR imaging techniques such as MR spectroscopy, diffusion-weighted, perfusion imaging and functional MR imaging, can provide relevant diagnostic information; however, they cannot be applied to whole-body imaging. Specific imaging sequences may have to be restricted to organs and body sections that benefit most from such imaging protocols (Fig. 3) [31].

A whole-body examination can be performed with five bed positions covering the head, neck, thorax, abdomen, and pelvis up to the thighs. Each bed position typically lasts 3–4 min to acquire the PET component, leading to a whole-body examination time of about 15–20 min for PET data. Strictly adhering to the time duration of PET acquisition, only 2 or at most 3 MR sequences can be obtained at each bed position. If one employs a normal diagnostic, yet still abridged, MR scan of the whole body; about 60–90 min is needed to cover all this territory with a sufficient range of MR sequences.

Optimized pulse sequences must provide at least as much information as low-dose unenhanced CT studies. This is usually done with three-dimensional T1-weighted 2-point Dixon that takes approximately 20 s per image stack and position. In fact, fat-suppressed T1-weighted images look very similar to pre-contrast CT images, with the major visual difference being that cortical bone. The use of Dixon sequences alone, for both AC and anatomic localization (Fig. 4), without additional MR sequences, can be done quickly enough to compete with PET-CT [32]; however, this method does not adequately utilize the added value of MRI [30]. One study compared the diagnostic performance of MR-PET against PET-CT by using a short examination time (<20 min) and using Dixon sequences for both, AC and anatomic localization [32], showing comparable reliability of MR-PET and PET-CT without significant differences regarding lesion detection. Tracer uptake in lesions and background correlated well between MR-PET and PET-CT. One subsequent study by Jeong et al. [33] compared the Dixon sequence on hybrid MR-PET with contrast-enhanced PET-CT for PET-positive lesions in patients with oncologic diseases. SUVs of PET-positive lesions correlated well between MR-PET and contrast-enhanced PET-CT; however, Dixon images provided less anatomic information of PET images, recommending additional MR sequences to improve anatomic information (Fig. 5).

In our approach to the MR-PET workflow, we currently use a combination of whole-body imaging based on pre-contrast and post-contrast imaging using the Dixon sequence, radial T1-weighted 3D-GRE, short-tau inversion recovery (STIR), T2-BLADE, or half-Fourier acquisition single-shot turbo spin-echo (HASTE) sequences; complemented by an organ-based imaging protocol. Depending on the body region of interest, a dedicated organ-based protocol is followed by a whole-body acquisition, which typically adds around 10 min to the total examination time. Pediatric patients represent a particular population where the imaging protocols for MR-PET should be kept as simple as possible to maintain patient tolerance. Free-breathing radial techniques, such as radial 3D GRE (T1-weighted) or BLADE (T2-weighted) are preferred, especially for the thoracic region and upper abdomen because their robustness to motion and due to the possibility of being acquired in a free-breathing fashion along the PET acquisition. Our approach for fusion of MR and PET data is based on the fact that PET data is acquired in a free-breathing manner, while many of the MR sequences we employ in MRI are breath-hold; therefore, as a result we have

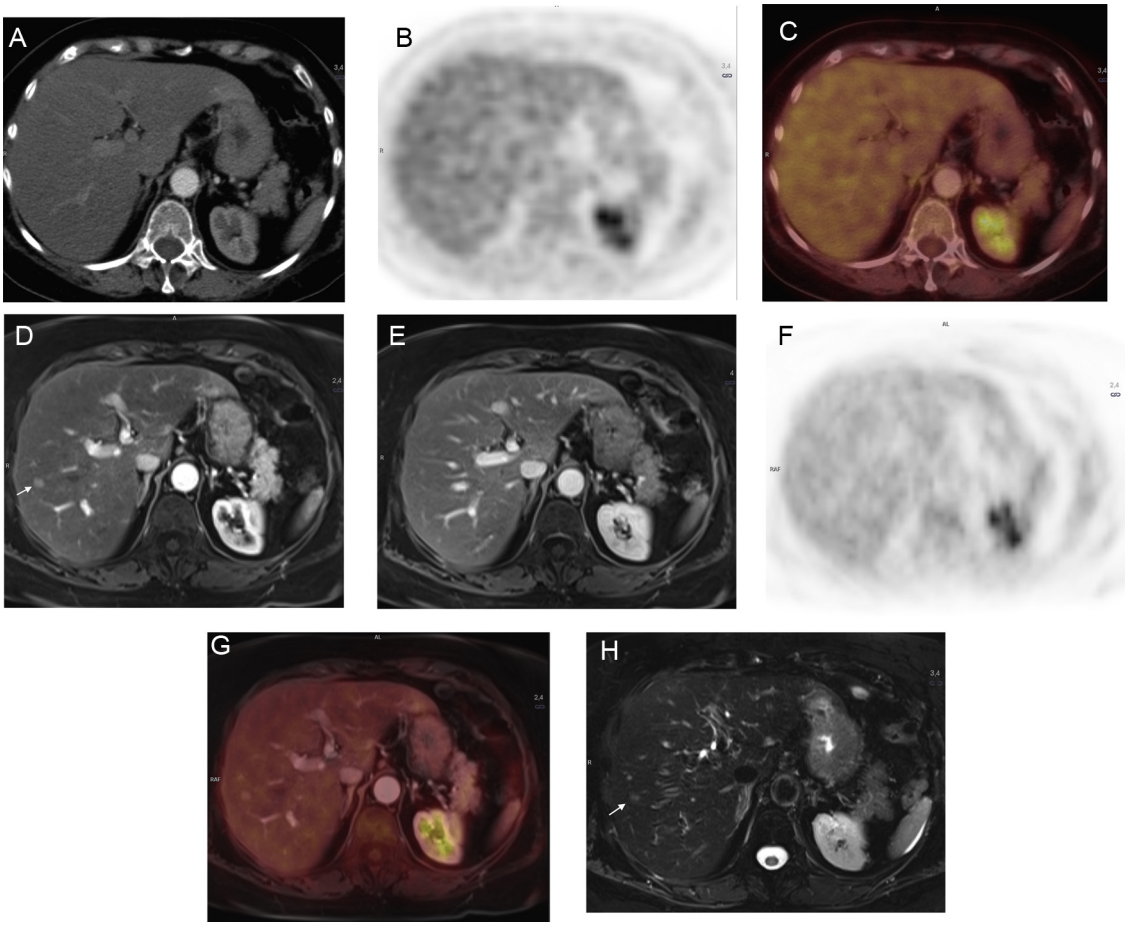


Fig. 2. Colorectal cancer follow-up. Axial contrast-enhanced CT (A), PET (B), and PET-CT (C) images. Axial contrast-enhanced T1-weighted VIBE MR on the arterial (D) and portal phase (E), PET (F); fused PET-T1-weighted VIBE MR (G), Fat-suppressed T2 TSE (H). A new solitary hypervascular liver lesion is seen between segments # VII and # VIII on MR images (D, F). The combination of mild T2-signal intensity (arrow, H), arterial hyper-enhancement (arrow, D) and fading in portal phase allowed the diagnosis of metastasis. This lesion is not seen on contrast-enhanced CT (A). PET images do not contribute to diagnostic accuracy.

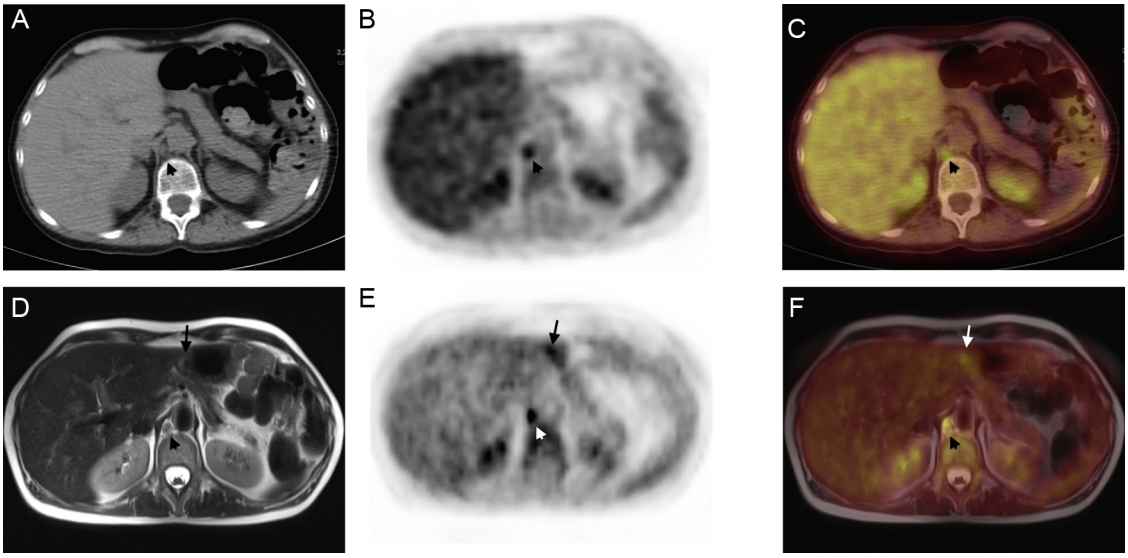


Fig. 3. Distal metastasis in a patient with recurrent ovarian cancer post-surgery. Axial unenhanced CT (A), PET (B), and PET-CT (C) images. Axial T2-weighted HASTE MR (D), PET (E), and Axial fused PET-T2-weighted HASTE MR (F). There is a small, round right retrocrural lymph node, which is appreciated on CT and MRI, and demonstrates intense FDG uptake on both PET acquisitions (arrowhead, A–F) in keeping with nodal metastasis. There is also a focal area of mildly increased signal intensity on HASTE, with corresponding focus of intense FDG uptake on the PET acquired with MR, involving the submucosal of the gastric antrum (arrow, D–F) suspicious for submucosal gastric metastasis. There is no corresponding CT or CT PET abnormality (A–C). Patient also has significant, FDG-avid, local recurrent disease (not shown).

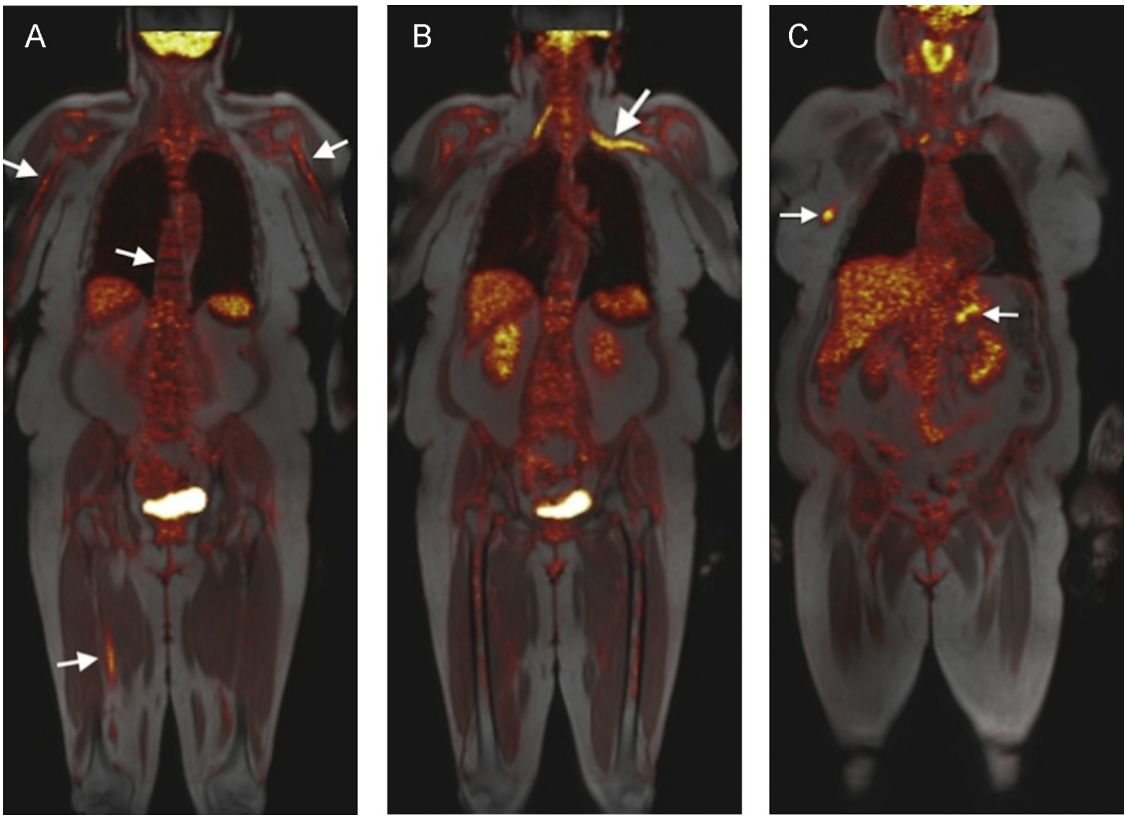


Fig. 4. Relapse of acute myeloid leukemia (AML) after haploidentical allogeneic stem cell transplant. Coronal fused MR-PET with in-phase 2-point Dixon images from attenuation correction sequences (A–C). Intense uptake is seen with diffuse replacement of bone marrow (arrows, A). The patient has also leukemic nerve involvement at the brachial plexus, which is more pronounced at the right (arrow, B). Pancreatic and mammary involvement were already depicted (arrow, C). Note the excellent registration between the two modalities.

incorporated novel breathing-averaged MR sequences for the purpose of accurate data fusion (see next section).

Other strategies of data acquisition are described in the literature for reference [26,27,29,34–37].

## 5. Motion correction

The expected benefit of an integrated MR-PET system requires adequate superimposition of image data sets, as

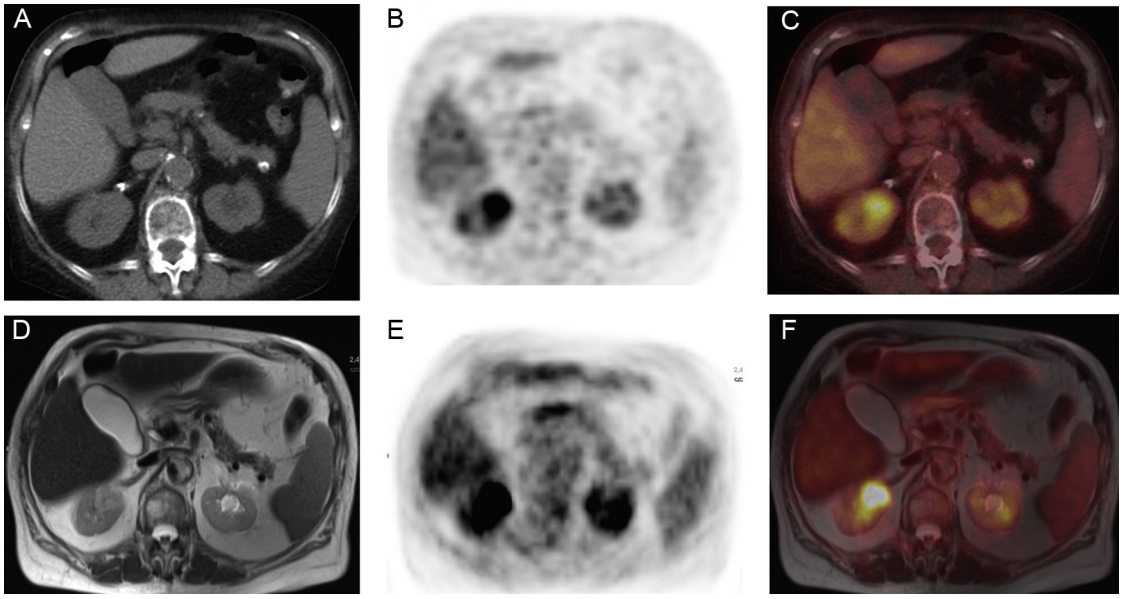


Fig. 5. Incidental renal cancer. Axial unenhanced CT (A), PET (B), and PET-CT (C) images. Axial T2-weighted HASTE MR (D), PET (E); fused PET-T2-weighted HASTE MR (F). A right kidney mass show intense uptake in both PET datasets (B, E). This lesion is not apparent on unenhanced CT (A), and improved delineation in seen on HASTE MR (D). Fused PET-CT (C) and MR-PET (F) confirm the malignant nature.

precise anatomic correlation between tracer-avid tissue and the anatomic detail derived from MRI images is necessary [26]. Registration software continues to evolve, but still at present do not achieve satisfactory results, especially in the body [38]. Software fusion of PET and MR images suffer from limitations, such as partial volume effects, different spatial resolutions between MR and PET, and physiologic motion with non-rigid structures. The fusion of brain images is relatively straightforward owing to its rigid structure (i.e., only rotation and translation) and lack of breathing-related or cardiac-related motion artifact. The territories that experience the greatest challenge for fusion are regions that represent non-rigid structures (i.e., can change shape) that experience physiologic motion, such as the thorax, abdomen and pelvis [39–41].

Manual re-registration of the upper abdomen can be challenging because of the relative paucity of internal landmarks [42,43].

To correct for the motion that abdominal organs undergo during respiration, several strategies have been described [44–46]. Free-breathing PET data acquisition is the standard approach for whole-body examinations on PET-CT and MR-PET. Historically, free-breathing acquisition is not ideal for MR sequences, which are sensitive to motion artifact. The trend of body MRI for the last 20 years has been to move toward breath-hold or single-shot type sequences, to minimize motion. Pairing free-breathing PET data with acquisition of MR data at the end of quiet expiration (similar to what it is done with PET-CT) might be one solution, as it has been shown with PET-CT to result in only minor misregistration. This strategy might be accomplished with breath-hold sequences such as T1-weighted 3D volumetric interpolated breath-held examination (VIBE) and fast spin echo T2-weighted sequences or with respiratory gated or navigated T2-weighted and diffusion-weighted images (DWI). Respiratory-gated T1-weighted sequences are feasible, but require unacceptably long acquisition times [47]. T2-weighted sequences may be acquired in a free-breathing manner with reasonable image quality using a snap shot type sequence such as HASTE; however, unpredictable misregistration between slices occur, if navigator-triggered pulses are not employed. Other sequences that can be acquired in a free-breathing manner and with acceptable image quality include free-breathing STIR and DWI, but they are also subjected to unpredictable misregistration between slices.

A further approach is the use of respiratory-gated acquisition of PET data [48–51]. However, this form of motion correction generates a final image that is reconstructed from only a portion of the total useful counts. The end result is an image that either suffers from reduced SNR or requires a very long acquisition to recoup counts and image quality, making this option inefficient for whole-body imaging [20].

Ongoing research evaluates other approaches, which include: a navigated 3D-GRE T1-weighted experimental sequence [47,52,53]. This technique acquires data when the navigator-determined position of the diaphragm falls within the acceptance window positioned during end-expiration. Cautious assessment of navigated techniques was provided by Brendle et al. [54], who showed that MR-based gated PET with end-expiratory attenuation correction map did not improve the alignment quality, but instead added a higher noise level.

The option we favor is the use of MR sequences that are obtained during free breathing but experience higher imager quality through the use of radial *k*-space filling of data and do not require demanding motion compensation methods. Other investigators have validated this approach; Rakheja et al. [55] showed that MR-PET using T1-weighted radial 3D-GRE sequences had more accurate spatial registration than PET-CT images. This is likely attributable both to the simultaneous acquisition of PET and MR data in a whole-body MR-PET system, compared to the sequential acquisition in a PET-CT system.

## 6. Comparison with PET-CT and early clinical experience in body applications

Potential clinical applications of MR-PET in body imaging include predominantly the fields of adult and pediatric oncology where PET-CT is already established. In terms of workflow and logistics, MR-PET offers the prospect to spare one additional examination. Nonetheless, it has to be evaluated which patient population is suitable for this new hybrid modality. Certainly, some patients will profit from this new imaging modality, such as children or young adults with anticipated multiple follow-up studies; as in patients with Hodgkin's disease, malignant melanoma, or sarcoma, in strive to reduce radiation exposure. Other application fields, such as neurology, cardiovascular disease, and therapy planning and response monitoring are now under initial evaluation. Current efforts in determining the performance of MR-PET in oncologic imaging focus on the prospective intra-individual comparison with PET-CT [26]. Initial results have been very encouraging, indicating some advantages for MR-PET, but almost all showing at least equivalent diagnostic performance to PET-CT.

In this section, we briefly review some of the current evidence regarding the comparison of MR-PET with PET-CT in various oncologic processes.

## 7. General oncology

In oncology, PET-CT is the mainstay in routine clinical practice. Given the very recent clinical accessibility of MR-PET, limited data is still available regarding the diagnostic performance of MR-PET for selected clinical indications [32,56–59]. Overall lesion detection rates in these studies showed high correlation values for detection of PET-positive lesions in PET-CT as well as MR-PET [32,56–59]. Quantification of lesion activity with PET-CT compared with MR-PET, showed in some studies lower SUVs for MR-PET. Potential reasons for these differences are inherent to the study design: In all comparison studies PET-CT has been performed first, then followed by MR-PET. Consequently, the advanced tracer metabolism and bio-distribution over time might have had an influence on lesion quantification. Another potential source of error is the MR-based AC [60]. Nevertheless, a recent study by Al-Nabhani et al. [61] showed no significant qualitative or quantitative differences between MR-PET and PET-CT. The PET data on both

modalities were similar; furthermore, they observed superior soft-tissue resolution of MR imaging in head and neck, pelvis, and colorectal cancers; and of CT in lung and mediastinal nodal disease, pointed to future tailored use in these locations.

A major concern in staging is the detection of lung metastasis or lung cancer staging and follow-up, since CT is known to be superior to MRI in the evaluation of the lung parenchyma [62]. Initial results are available on direct comparison between MR-PET and PET-CT in the staging of lung cancer, mostly non-small-cell lung cancer; however, many of these studies are limited by small sample size [63–65]. Schwenzer et al. [63] reported on ten patients with lung cancer and compared PET-CT with MR-PET, and concluded that lesion characterization and tumor detection were similar in most patients.

The performance of MR-PET has also been studied for the detection of pulmonary nodules [66]. Using simultaneous PET and a free-breathing T1-weighted radial 3D-GRE, the detection of pulmonary nodules was compared with that of PET-CT. A total of 69 nodules, including 45 FDG-avid lesions, were detected. The sensitivity of MR-PET was 70.3% for all nodules, 95.6% for FDG-avid nodules, and 88.6% for nodules 0.5 cm in diameter or larger. There was a significantly strong correlation between SUV quantitative data of pulmonary nodules obtained with PET-CT and that obtained with MR-PET ($r = 0.96$, $p < 0.001$).

A recent study comparing PET-CT and MR-PET demonstrated the effectiveness of whole-body MR-PET in oncology [61] showing no significant differences between MR-PET and PET-CT in regard to confidence and degree of agreement of anatomic lesion localization. In this study 227 tracer-avid lesions were identified in 50 patients. MR-PET imaging identified 2 additional lesions. There was 10% improvement in local staging with MR-PET. The alignment was better for MR-PET imaging.

In another study, Pace et al. [67] compared whole-body PET-CT and MR-PET regarding lesion detection and quantitation of FDG uptake in lesions and in normal organ tissues in breast cancer patients. Their study demonstrated that whole-body MR-PET was feasible in that clinical setting. MR-PET showed equivalent performance to PET-CT and SUV measurements correlated well (Fig. 6).

One study by Catalano et al. [68] compared the clinical impact of combined MR-PET to that of combined PET-CT. The studies were performed in 134 patients with cancer, and showed that findings affecting clinical management were noted for PET-CT studies but not for MR-PET studies in 2/134 patients, and for MR-PET studies but not for PET-CT studies in 24/134 patients. MR-PET contributed to clinical management more often than did PET-CT.

Intra-individual studies for specific conditions appear in fewer numbers. In a study with 70 patients, Beiderwellen et al. [69] assessed the value of MR-PET using a whole-body protocol for the depiction and characterization of liver lesions in comparison to PET-CT. They concluded that MR-PET, even in the setting of a whole-body approach, provided higher lesion conspicuity and diagnostic confidence, and might therefore evolve as an alternative in oncologic imaging. Gaertner et al. [70] compared a short protocol using Dixon sequences for AC and anatomic localization and compared $^{68}$Ga-DOTATOC MR-PET with PET-CT in patients with neuroendocrine tumors. The SUVs of focal lesions did not differ between the PET-CT and MR-PET acquisitions, and correlated in a linear fashion ($\rho = 0.90$) and the detectability of focal PET lesions was equivalent to PET-CT on a patient basis and organ system basis.

Concerning the evaluation of malignant bone lesions (Fig. 7), Eiber et al. [71] showed that whole-body MR-PET is technically and clinically robust for evaluation of bone lesions. Ninety-eight bone lesions were identified in 33 of 119 patients. Visual lesion conspicuity was comparable for PET-CT and MR-PET. For bone lesions and regions of normal bone, a highly significant correlation occurred between the mean SUVs for MR-PET and PET-CT ($r = 0.950$ and 0.917, respectively). MR-PET, including diagnostic T1-weighted TSE sequences, was superior to PET-CT for anatomic delineation and allocation of bone lesions. These observations might be of clinical relevance in selected cases, such as in primary bone tumors and in routine oncologic protocol for MR-PET.

One of the strongest evidence for a clinical indication of MR-PET occurs in the head and neck cancer population (Fig. 8). Due to frequent distant metastases the whole body approach of hybrid MR-PET may be an advantage. Kuhn et al. [72] compared contrast-enhanced MR-PET imaging with contrast-enhanced PET-CT in 150 consecutive patients referred for primary staging or restaging of head and neck cancer. MR-PET had comparable image quality to CT and MR, and T2-weighted MR-PET imaging performed similarly, for metastatic lymph nodes, or better than contrast-enhanced PET/CT, for primary tumors, in the morphologic characterization of PET-positive lesions. Study results provided evidence that MR-PET imaging could serve as a legitimate alternative to PET-CT in the clinical workup of patients with head and neck cancers. These results are particularly important, as the interfaces between bone, air, and soft tissues in nasopharynx, oropharynx, and hypopharynx are considered major challenges for MR-PET.

## 8. Pediatric oncology

The use of PET-CT in pediatric oncology has increased dramatically in the past decade. The main indications include staging and monitoring of lymphomas, sarcomas, nasopharyngeal carcinoma, neuroblastoma, CNS-tumors, cancer of unknown primary, and radiotherapy planning [34]. Additionally, MR-PET can be an alternative to PET-CT for longitudinal follow-up studies monitoring the therapeutic response to chemotherapy.

MR-PET can be seen as a valuable alternative to PET-CT, especially in pediatric population. The substitution of PET-CT by MR-PET in these patients reduces the overall dose by the fraction of the CT scan multiplied by the individual necessary number of follow-up examinations per patient, while preserving the advantages of hybrid imaging [17,34]. Potential dose savings of up to 80% have been postulated when using MR-PET instead of PET-CT in pediatric oncologic imaging [35]. Patient exposure to radiation from complementary CT is a major

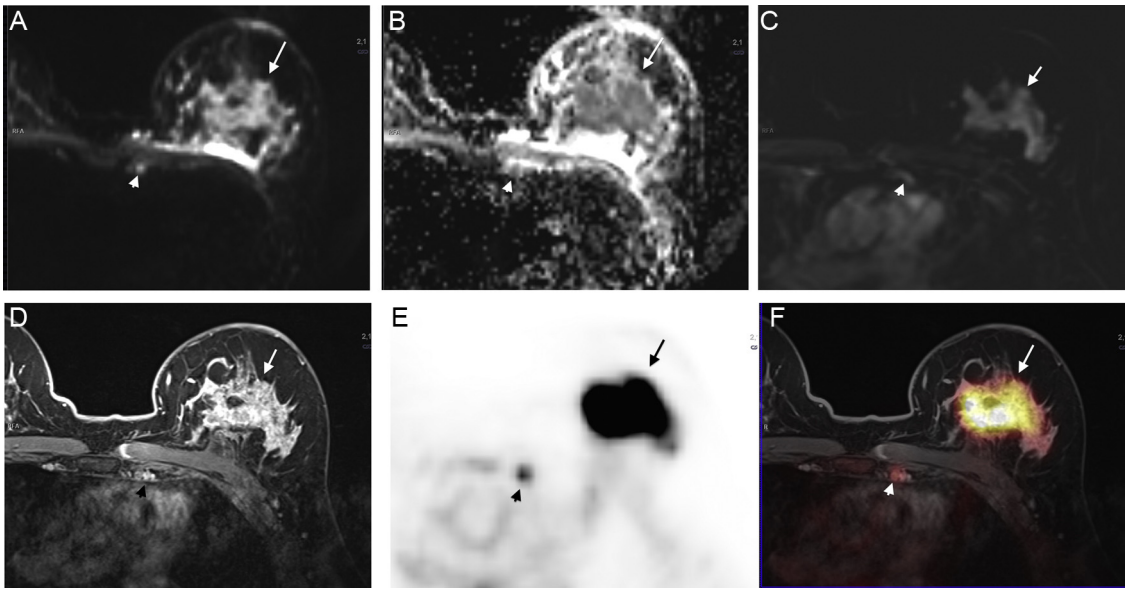


Fig. 6. Large left breast cancer with nodal metastasis. Axial DWI (A), ADC map (B), axial subtraction dynamic post-gadolinium 3D-GRE fat-suppressed T1-weighted image (C), and axial post-gadolinium 3D-GRE fat-suppressed T1-weighted image (D). Axial PET (E) and fused PET-T1-weighted VIBE MR (F) images. There is a large irregular mass involving the central region of the left breast, which demonstrates increased signal on the DWI (arrow, A) and low signal on the ADC map (arrow, B) images, in keeping with a true restriction. The mass demonstrates intense enhancement (arrow, C–D), intense FDG uptake (arrow, E), in keeping with aggressive breast cancer. There is also a small round ipsilateral internal mammary lymph node, which demonstrates similar signal characteristics and FDG uptake to that of the primary breast mass (arrowhead, A–F) in keeping with a metastatic nodal disease. Patient also has evidence of ipsilateral axillary nodal metastatic disease (not shown).

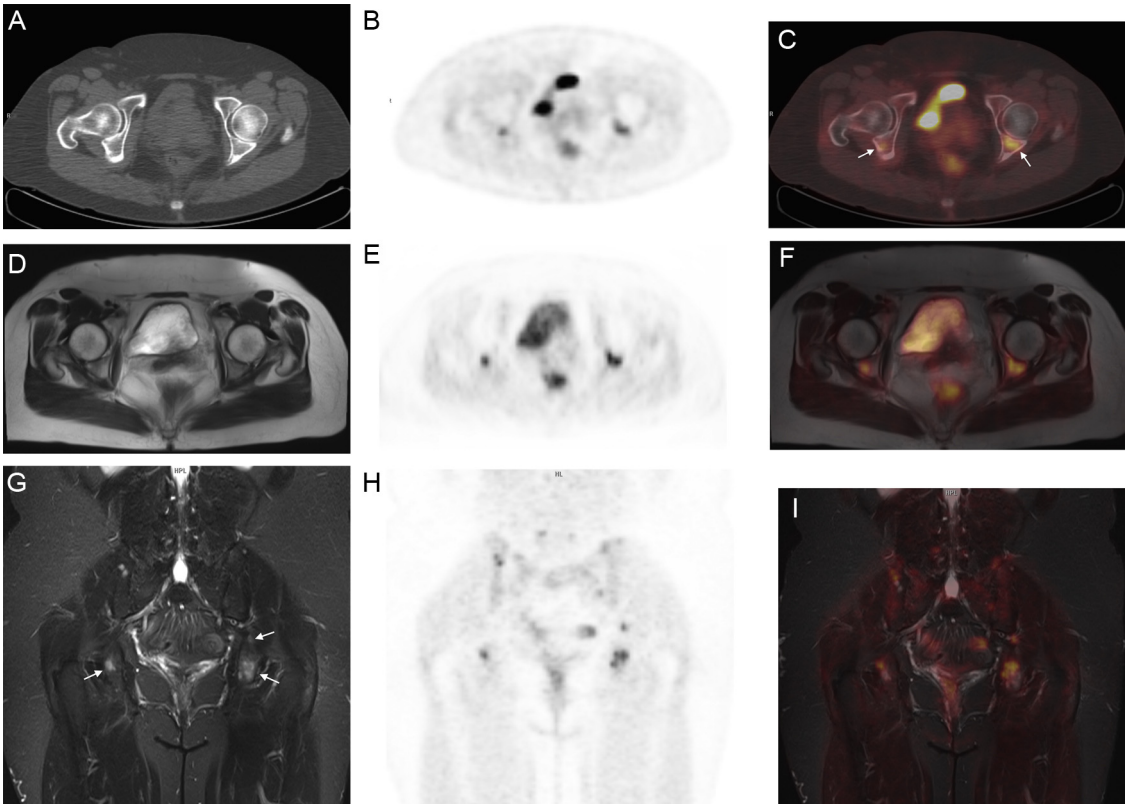


Fig. 7. Images of bone metastases in a patient with breast cancer. Axial unenhanced CT (A), PET (B), and PET-CT (C) images. Axial T2-weighted HASTE MR (D), PET (E); fused PET-T2-weighted HASTE MR (F). Coronal STIR (G), PET (H), fused PET-STIR MR (I). Two bone metastases in the posterior acetabulum showing intense uptake are seen on PET and PET-CT (arrows, C) and MR-PET. Equivalent detectability is perceived between unenhanced CT and HASTE datasets (A and D). STIR images show improved morphologic characterization of PET-positive lesions (arrows, G).

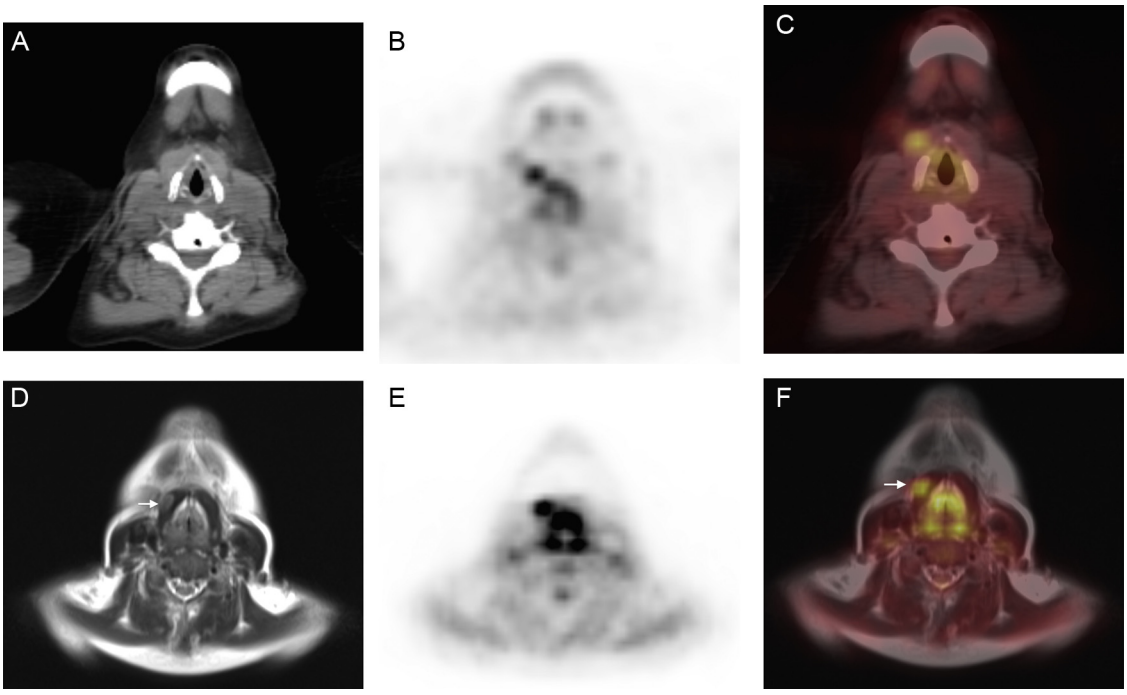


Fig. 8. Status post thyroidectomy in a patient with elevated thyroxine-binding globulin levels. Axial unenhanced CT (A), PET (B), and PET-CT (C) images. Axial T2-weighted HASTE MR (D), PET (E), fused PET-T2-weighted HASTE MR (F). A mildly T2-weighted hyperintense nodule is seen adjacent to the right aspect of the thyroid cartilage, involving the omohyoid/sternohyod muscles (arrow, D). This nodule is not seen on unenhanced CT images (A). Fused PET-CT and PET-MR show good anatomic correlation of the cervical nodule with increased activity (B, E) of this nodule a. HASTE images show improved morphologic characterization of PET-positive lesions (arrows, D).

concern in pediatrics, due to the risk of developing secondary cancer [73–76] as survival of children with cancer has increased considerably.

Although this is a new application and data are still sparse, the first indications support that MR-PET is a promising modality for the clinical work-up of pediatric malignancies [35,77–79]. Schuler et al. [80] presented their first experiences using combined MR-PET for high-risk sarcomas. MR-PET contributed to decision-making, and helped to guide biopsies of large and heterogeneous tumors. Another study evaluating co-registration of PET and MRI datasets for staging of pediatric cancers, found MR-PET to be the methodology of choice for adequate of single tumor detection and staging [81].

Prospective studies are needed comparing staging accuracy of MR-PET to that of PET-CT using the same radiotracer. Schäfer et al. [82] compared MR-PET and PET-CT for lesion detection and interpretation, as well as quantification of FDG uptake and accuracy of MR-PET in pediatric patients with solid tumors. They showed that MR-PET was technically feasible; with satisfactory performance for PET quantification with SUVs similar to those of PET-CT. MR-PET demonstrated equivalent lesion detection rates while offering markedly reduced radiation exposure.

## 9. Conclusion

MR-PET is a recent technique that offers the possibility to assess anatomic, functional, and metabolic information in one examination. Although it offers the additional advantage of radiation-reduced examination, it needs to be further evaluated against PET-CT. It is also important to evaluate if combined MR-PET scanners are economical viable compared to individual systems.

In order to achieve optimum impact and ensure clinical acceptance of this exciting new technology, defined MR-PET protocols are necessary to make MR-PET fast enough to compete with PET-CT, while providing additional clinical value over PET-CT.

Current evidence shows overall good correlation between PET-CT and MR-PET in lesion detection across most publications on oncologic diseases. Moreover, initial results in pediatric patients are encouraging, particularly with the reduction in radiation exposure.

## Conflict of interest

None.

## References

[1] Catana C, Procissi D, Wu Y, Judenhofer MS, Qi J, Pichler BJ, et al. Simultaneous in vivo positron emission tomography and magnetic resonance imaging. Proc Natl Acad Sci U S A 2008;105:3705–10.
[2] Judenhofer MS, Wehrl HF, Newport DF, Catana C, Siegel SB, Becker M, et al. Simultaneous PET-MRI: a new approach for functional and morphological imaging. Nat Med 2008;14:459–65.
[3] Hany TF, Steinert HC, Goerres GW, Buck A, Schulthess von GK. PET diagnostic accuracy: improvement with in-line PET-CT system: initial results. Radiology 2002;225:575–81.

[4] Schulthess von GK, Hany TF. Imaging and PET-PET/CT imaging. J Radiol 2008;89:438–47, quiz448.
[5] Maziak DE, Darling GE, Inculet RI, Gulenchyn KY, Driedger AA, Ung YC, et al. Positron emission tomography in staging early lung cancer: a randomized trial. Ann Intern Med 2009;151:221–8. W-48.
[6] Ben-Haim S, Ell P. 18F-FDG PET and PET/CT in the evaluation of cancer treatment response. J Nucl Med 2009;50:88–99.
[7] Slates RB, Farahani K, Shao Y, Marsden PK, Taylor J, Summers PE, et al. A study of artefacts in simultaneous PET and MR imaging using a prototype MR compatible PET scanner. Phys Med Biol 1999;44:2015–27.
[8] Hofmann M, Bezrukov I, Mantlik F, Aschoff P, Steinke F, Beyer T, et al. MRI-based attenuation correction for whole-body PET/MRI: quantitative evaluation of segmentation- and atlas-based methods. J Nucl Med 2011;52:1392–9.
[9] Martinez-Moller A, Souvatzoglou M, Delso G, Bundschuh RA, Chefd'hotel C, Ziegler SI, et al. Tissue classification as a potential approach for attenuation correction in whole-body PET/MRI: evaluation with PET/CT data. J Nucl Med 2009;50:520–6.
[10] Hofmann M, Steinke F, Scheel V, Charpiat G, Farquhar J, Aschoff P, et al. MRI-based attenuation correction for PET/MRI: a novel approach combining pattern recognition and atlas registration. J Nucl Med 2008;49:1875–83.
[11] Schulthess von GK, Kuhn FP, Kaufmann P, Veit-Haibach P. Clinical positron emission tomography/magnetic resonance imaging applications. Semin Nucl Med 2013;43:3–10.
[12] Mansi L, Ciarmiello A, Cuccurullo V. PET/MRI and the revolution of the third eye. Eur J Nucl Med Mol Imaging 2012;39:1519–24.
[13] Yankeelov TE, Peterson TE, Abramson RG, Izquierdo-Garcia D, Arlinghaus LR, Li X, et al. Simultaneous PET-MRI in oncology: a solution looking for a problem? Magn Reson Imaging 2012;30:1342–56.
[14] Herzog H, Van Den Hoff J. Combined PET/MR systems: an overview and comparison of currently available options. Q J Nucl Med Mol Imaging 2012;56:247–67.
[15] Herzog H. PET/MRI: challenges, solutions and perspectives. Z Med Phys 2012;22:281–98.
[16] Kalemis A, Delattre BMA, Heinzer S. Sequential whole-body PET/MR scanner: concept, clinical use, and optimisation after two years in the clinic. The manufacturer's perspective. MAGMA 2013;26:5–23.
[17] Delso G, Fürst S, Jakoby B, Ladebeck R, Ganter C, Nekolla SG, et al. Performance measurements of the Siemens mMR integrated whole-body PET/MR scanner. J Nucl Med 2011;52:1914–22.
[18] Bezrukov I, Mantlik F, Schmidt H, Scholkopf B, Pichler BJ. M.R-based PET attenuation correction for PET/MR imaging. Semin Nucl Med 2013;43:45–59.
[19] Schulz V, Torres-Espallardo I, Renisch S, Hu Z, Ojha N, Bornert P, et al. Automatic, three-segment, MR-based attenuation correction for whole-body PET/MR data. Eur J Nucl Med Mol Imaging 2011;38:138–52.
[20] Fowler KJ, McConathy J, Narra VR. Whole-body simultaneous positron emission tomography (PET)-MR: optimization and adaptation of MRI sequences. J Magn Reson Imaging 2014;39:259–68.
[21] Hofmann M, Pichler B, Scholkopf B, Beyer T. Towards quantitative PET/MRI: a review of MR-based attenuation correction techniques. Eur J Nucl Med Mol Imaging 2009;36(Suppl. 1):S93–104.
[22] Keereman V, Mollet P, Berker Y, Schulz V, Vandenberghe S. Challenges and current methods for attenuation correction in PET/MR. MAGMA 2013;26:81–98.
[23] Andersen FL, Ladefoged CN, Beyer T, Keller SH, Hansen AE, Hojgaard L, et al. Combined PET/MR imaging in neurology: MR-based attenuation correction implies a strong spatial bias when ignoring bone. Neuroimage 2014;84:206–16.
[24] Bailey DL, Barthel H, Beuthin-Baumann B, Beyer T, Bisdas S, Boellaard R, et al. Combined PET/MR: where are we now? Summary report of the second international workshop on PET/MR imaging April 8–12, 2013, Tubingen, Germany. Mol Imaging Biol 2014;16:295–310.
[25] Reiner CS, Stolzmann P, Husmann L, Burger IA, Hullner MW, Schaefer NG, et al. Protocol requirements and diagnostic value of PET/MR imaging for liver metastasis detection. Eur J Nucl Med Mol Imaging 2014;41:649–58.
[26] Schwenzer NF, Schmidt H, Claussen CD. Whole-body MR/PET: applications in abdominal imaging. Abdom Imaging 2012;37:20–8.
[27] Werner MK, Schmidt H, Schwenzer NF. MR/PET: a new challenge in hybrid imaging. Am J Roentgenol 2012;199:272–7.
[28] Eiber M, Souvatzoglou M, Pickhard A, Loeffelbein DJ, Knopf A, Holzapfel K, et al. Simulation of a MR-PET protocol for staging of head-and-neck cancer including Dixon MR for attenuation correction. Eur J Radiol 2012;81:2658–65.
[29] Martinez-Moller A, Eiber M, Nekolla SG, Souvatzoglou M, Drzezga A, Ziegler S, et al. Workflow and scan protocol considerations for integrated whole-body PET/MRI in oncology. J Nucl Med 2012;53:1415–26.
[30] Herrmann K, Kohan A, Gaeta M, Rubbert C, Vercher-Conejero J, Paspulati R, et al. PET/MRI: applications in clinical imaging. Curr Radiol Rep 2013;1:161–76.
[31] Ratib O, Beyer T. Whole-body hybrid PET/MRI: ready for clinical use? Eur J Nucl Med Mol Imaging 2011;38:992–5.
[32] Drzezga A, Souvatzoglou M, Eiber M, Beer AJ, Fürst S, Martinez-Moller A, et al. First clinical experience with integrated whole-body PET/MR: comparison to PET/CT in patients with oncologic diagnoses. J Nucl Med 2012;53:845–55.
[33] Jeong JH, Cho IH, Kong EJ, Chun KA. Evaluation of Dixon sequence on hybrid PET/MR compared with contrast-enhanced PET/CT for PET-positive lesions. Nucl Med Mol Imaging 2014;48:26–32.
[34] Kjaer A, Loft A, Law I, Berthelsen AK, Borgwardt L, Lofgren J, et al. PET/MRI in cancer patients: first experiences and vision from Copenhagen. MAGMA 2013;26:37–47.
[35] Hirsch FW, Sattler B, Sorge I, Kurch L, Viehweger A, Ritter L, et al. PET/MR in children. Initial clinical experience in paediatric oncology using an integrated PET/MR scanner. Pediatr Radiol 2013;43:860–75.
[36] Schulthess von GK, Veit-Haibach P. Workflow considerations in PET/MR imaging. J Nucl Med 2014;55:19S–24S.
[37] Vargas M-I, Becker M, Garibotto V, Heinzer S, Loubeyre P, Gariani J, et al. Approaches for the optimization of MR protocols in clinical hybrid PET/MRI studies. MAGMA 2013;26:57–69.
[38] Judenhofer MS, Cherry SR. Applications for preclinical PET/MRI. Semin Nucl Med 2013;43:19–29.
[39] Schwarz AJ, Leach MO. Implications of respiratory motion for the quantification of 2D MR spectroscopic imaging data in the abdomen. Phys Med Biol 2000;45:2105–16.
[40] Dawood M, Buther F, Stegger L, Jiang X, Schober O, Schafers M, et al. Optimal number of respiratory gates in positron emission tomography: a cardiac patient study. Med Phys 2009;36:1775–84.
[41] Suramo I, Paivansalo M, Myllyla V. Cranio-caudal movements of the liver, pancreas and kidneys in respiration. Acta Radiol Diagn (Stockh) 1984;25:129–31.
[42] Forster GJ, Laumann C, Nickel O, Kann P, Rieker O, Bartenstein P. SPET/CT image co-registration in the abdomen with a simple and cost-effective tool. Eur J Nucl Med Mol Imaging 2003;30:32–9.
[43] Slomka PJ, Dey D, Przetak C, Aladl UE, Baum RP. Automated 3-dimensional registration of stand-alone (18)F-FDG whole-body PET with CT. J Nucl Med 2003;44:1156–67.
[44] Grimm R, Fürst S, Dregely I, Forman C, Hutter JM, Ziegler SI, et al. Self-gated radial MRI for respiratory motion compensation on hybrid PET/MR systems. Med Image Comput Comput Assist Interv 2013;16:17–24.
[45] Guerin B, Cho S, Chun SY, Zhu X, Alpert NM, Fakhri El G, et al. Non-rigid PET motion compensation in the lower abdomen using simultaneous tagged-MRI and PET imaging. Med Phys 2011;38:3025–38.
[46] Wurslin C, Schmidt H, Martirosian P, Brendle C, Boss A, Schwenzer NF, et al. Respiratory motion correction in oncologic PET using T1-weighted MR imaging on a simultaneous whole-body PET/MR system. J Nucl Med 2013;54:464–71.
[47] Lee ES, Lee JM, Yu MH, Shin C-I, Woo HS, Joo I, et al. High spatial resolution, respiratory-gated, t1-weighted magnetic resonance imaging of the liver and the biliary tract during the hepatobiliary phase of gadoxetic acid-enhanced magnetic resonance imaging. J Comput Assist Tomogr 2014;38:360–6.

[48] Fin L, Daouk J, Morvan J, Bailly P, Esper El I, Saidi L, et al. Initial clinical results for breath-hold CT-based processing of respiratory-gated PET acquisitions. Eur J Nucl Med Mol Imaging 2008;35:1971–80.
[49] Fin L, Daouk J, Bailly P, Slama J, Morvan J, Esper El I, et al. Improved imaging of intrahepatic colorectal metastases with 18F-fluorodeoxyglucose respiratory-gated positron emission tomography. Nucl Med Commun 2012;33:656–62.
[50] Daouk J, Leloire M, Fin L, Bailly P, Morvan J, Esper El I, et al. Respiratory-gated 18F-FDG PET imaging in lung cancer: effects on sensitivity and specificity. Acta Radiol 2011;52:651–7.
[51] Chang G, Chang T, Pan T, Clark JWJ, Mawlawi OR. Implementation of an automated respiratory amplitude gating technique for PET/CT: clinical evaluation. J Nucl Med 2010;51:16–24.
[52] Kuhn J-P, Holmes JH, Brau ACS, Iwadate Y, Hernando D, Reeder SB. Navigator flip angle optimization for free-breathing T1-weighted hepatobiliary phase imaging with gadoxetic acid. J Magn Reson Imaging 2013, http://dx.doi.org/10.1002/jmri.24480 [Epub ahead of print].
[53] Nagle SK, Busse RF, Brau AC, Brittain JH, Frydrychowicz A, Iwadate Y, et al. High resolution navigated three-dimensional T(1)-weighted hepatobiliary MRI using gadoxetic acid optimized for 1.5 Tesla. J Magn Reson Imaging 2012;36:890–9.
[54] Brendle CB, Schmidt H, Fleischer S, Braeuning UH, Pfannenberg CA, Schwenzer NF. Simultaneously acquired MR/PET images compared with sequential MR/PET and PET/CT: alignment quality. Radiology 2013;268:190–9.
[55] Rakheja R, DeMello L, Chandarana H, Glielmi C, Geppert C, Faul D, et al. Comparison of the accuracy of PET/CT and PET/MRI spatial registration of multiple metastatic lesions. Am J Roentgenol 2013;201:1120–3.
[56] Buchbender C, Heusner TA, Lauenstein TC, Bockisch A, Antoch G. Oncologic PET/MRI, part 1: tumors of the brain, head and neck, chest, abdomen, and pelvis. J Nucl Med 2012;53:928–38.
[57] Boss A, Bisdas S, Kolb A, Hofmann M, Ernemann U, Claussen CD, et al. Hybrid PET/MRI of intracranial masses: initial experiences and comparison to PET/CT. J Nucl Med 2010;51:1198–205.
[58] Wiesmuller M, Quick HH, Navalpakkam B, Lell MM, Uder M, Ritt P, et al. Comparison of lesion detection and quantitation of tracer uptake between PET from a simultaneously acquiring whole-body PET/MR hybrid scanner and PET from PET/CT. Eur J Nucl Med Mol Imaging 2013;40:12–21.
[59] Quick HH, Gall von C, Zeilinger M, Wiesmuller M, Braun H, Ziegler S, et al. Integrated whole-body PET/MR hybrid imaging: clinical experience. Investig Radiol 2013;48:280–9.
[60] Quick HH. Integrated P.E.T/M.R. J Magn Reson Imaging 2014;39:243–58.
[61] Al-Nabhani KZ, Syed R, Michopoulou S, Alkalbani J, Afaq A, Panagiotidis E, et al. Qualitative and quantitative comparison of PET/CT and PET/MR imaging in clinical practice. J Nucl Med 2014;55:88–94.
[62] Biederer J, Hintze C, Fabel M. MRI of pulmonary nodules: technique and diagnostic value. Cancer Imaging 2008;8:125–30.
[63] Schwenzer NF, Schraml C, Muller M, Brendle C, Sauter A, Spengler W, et al. Pulmonary lesion assessment: comparison of whole-body hybrid MR/PET and PET/CT imaging – pilot study. Radiology 2012;264:551–8.
[64] Yi CA, Shin KM, Lee KS, Kim B-T, Kim H, Kwon OJ, et al. Non-small cell lung cancer staging: efficacy comparison of integrated PET/CT versus 3.0-T whole-body MR imaging. Radiology 2008;248:632–42.
[65] Schmidt H, Brendle C, Schraml C, Martirosian P, Bezrukov I, Hetzel J, et al. Correlation of simultaneously acquired diffusion-weighted imaging and 2-deoxy-[18F] fluoro-2-D-glucose positron emission tomography of pulmonary lesions in a dedicated whole-body magnetic resonance/positron emission tomography system. Investig Radiol 2013;48:247–55.
[66] Chandarana H, Heacock L, Rakheja R, DeMello LR, Bonavita J, Block TK, et al. Pulmonary nodules in patients with primary malignancy: comparison of hybrid PET/MR and PET/CT imaging. Radiology 2013;268:130620–881.
[67] Pace L, Nicolai E, Luongo A, Aiello M, Catalano OA, Soricelli A, et al. Comparison of whole-body PET/CT and PET/MRI in breast cancer patients: lesion detection and quantitation of 18F-deoxyglucose uptake in lesions and in normal organ tissues. Eur J Radiol 2014;83:289–96.
[68] Catalano OA, Rosen BR, Sahani DV, Hahn PF, Guimaraes AR, Vangel MG, et al. Clinical impact of PET/MR imaging in patients with cancer undergoing same-day PET/CT: initial experience in 134 patients – a hypothesis-generating exploratory study. Radiology 2013;269(3):857–69.
[69] Beiderwellen K, Gomez B, Buchbender C, Hartung V, Poeppel TD, Nensa F, et al. Depiction and characterization of liver lesions in whole body [(1)(8)F]-FDG PET/MRI. Eur J Radiol 2013;82:e669–75.
[70] Gaertner FC, Beer AJ, Souvatzoglou M, Eiber M, Fürst S, Ziegler SI, et al. Evaluation of feasibility and image quality of 68Ga-DOTATOC positron emission tomography/magnetic resonance in comparison with positron emission tomography/computed tomography in patients with neuroendocrine tumors. Investig Radiol 2013;48:263–72.
[71] Eiber M, Takei T, Souvatzoglou M, Mayerhoefer ME, Fürst S, Gaertner FC, et al. Performance of whole-body integrated 18F-FDG PET/MR in comparison to PET/CT for evaluation of malignant bone lesions. J Nucl Med 2014;55:191–7.
[72] Kuhn FP, Hullner M, Mader CE, Kastrinidis N, Huber GF, Schulthess von GK, et al. Contrast-enhanced PET/MR imaging versus contrast-enhanced PET/CT in head and neck cancer: how much MR information is needed? J Nucl Med 2014;55:551–8.
[73] Fahey FH, Treves ST, Adelstein SJ. Minimizing and communicating radiation risk in pediatric nuclear medicine. J Nucl Med 2011;52:1240–51.
[74] Lassmann M, Biassoni L, Monsieurs M, Franzius C, Jacobs F. The new EANM paediatric dosage card. Eur J Nucl Med Mol Imaging 2007;34:796–8.
[75] Lassmann M, Biassoni L, Monsieurs M, Franzius C. The new EANM paediatric dosage card: additional notes with respect to F-18. Eur J Nucl Med Mol Imaging 2008;35:1666–8.
[76] Pearce MS, Salotti JA, Little MP, McHugh K, Lee C, Kim KP, et al. Radiation exposure from CT scans in childhood and subsequent risk of leukaemia and brain tumours: a retrospective cohort study. Lancet 2012;380:499–505.
[77] Chavhan GB, Babyn PS. Whole-body MR imaging in children: principles, technique, current applications, and future directions. Radiographics 2011;31:1757–72.
[78] Goo HW, Choi SH, Ghim T, Moon HN, Seo JJ. Whole-body MRI of paediatric malignant tumours: comparison with conventional oncological imaging methods. Pediatr Radiol 2005;35:766–73.
[79] Kwee TC, Takahara T, Vermoolen MA, Bierings MB, Mali WP, Nievelstein RAJ. Whole-body diffusion-weighted imaging for staging malignant lymphoma in children. Pediatr Radiol 2010;40:1592–602, quiz1720–1.
[80] Schuler MK, Richter S, Beuthien-Baumann B, Platzek I, Kotzerke J, van den Hoff J, et al. PET/MRI imaging in high-risk sarcoma: first findings and solving clinical problems. Case Rep Oncol Med 2013;2013:793927.
[81] Pfluger T, Melzer HI, Mueller WP, Coppenrath E, Bartenstein P, Albert MH, et al. Diagnostic value of combined (1)(8)F-FDG PET/MRI for staging and restaging in paediatric oncology. Eur J Nucl Med Mol Imaging 2012;39:1745–55.
[82] Schäfer JF, Gatidis S, Schmidt H, Guckel B, Bezrukov I, Pfannenberg CA, et al. Simultaneous whole-body PET/MR imaging in comparison to PET/CT in pediatric oncology: initial results. Radiology 2014:131732.